Atomistic mechanisms of cyclic hardening in metallic glass

Chuang Deng and Christopher A. Schuh

Related Articles

Enhanced texture in die-upset nanocomposite magnets by Nd-Cu grain boundary diffusion
Appl. Phys. Lett. 102, 072409 (2013)

Tensile strained GeSn on Si by solid phase epitaxy
Appl. Phys. Lett. 102, 052106 (2013)

Systematic structural and chemical characterization of the transition layer at the interface of NO-annealed 4H-SiC/SiO2 metal-oxide-semiconductor field-effect transistors
J. Appl. Phys. 113, 044517 (2013)

Giant energy density in [001]-textured Pb(Mg1/3Nb2/3)O3-PbZrO3-PbTiO3 piezoelectric ceramics
Appl. Phys. Lett. 102, 042903 (2013)

Graphene–Fe3O4 nanohybrids: Synthesis and excellent electromagnetic absorption properties
J. Appl. Phys. 113, 024314 (2013)

Additional information on Appl. Phys. Lett.

Atomistic mechanisms of cyclic hardening in metallic glass

Chuang Deng[1,2,a)] and Christopher A. Schuh[2]

[1]*Department of Mechanical and Manufacturing Engineering, The University of Manitoba, 15 Gillson Street, Winnipeg, Manitoba R3T 5V6, Canada*

[2]*Department of Materials Science and Engineering, Massachusetts Institute of Technology, 77 Massachusetts Ave, Cambridge, Massachusetts 02139, USA*

Molecular dynamics with an embedded-atom method potential is used to simulate the nanoindentation of $Cu_{63.5}Zr_{36.5}$ metallic glasses. In particular, the effects of cyclic loading within the nominal elastic range on the overall strength and plasticity of metallic glass are studied. The simulated results are in line with the characteristics of experimentally observed hardening effects. In addition, analysis based on local von Mises strain suggests that the hardening is induced by confined microplasticity and stiffening in regions of the originally preferred yielding path, requiring a higher applied load to trigger a secondary one. © 2012 American Institute of Physics. [http://dx.doi.org/10.1063/1.4729941]

Whereas plasticity in crystalline materials can be well characterized based on dislocations, such a generalized framework does not yet exist for metallic glasses.[1] And while this lack of a structure-based model of plasticity poses some problems for understanding the onset of plasticity and its localization into shear bands once the yield stress is reached, it is especially troublesome when trying to physically rationalize more subtle mechanical properties. One of these is plastic damage evolution under cyclic loading. Despite their lack of dislocation substructure, which can evolve under cyclic loading and provide a source of kinematically irreversible damage accumulation in crystalline materials, metallic glasses still exhibit a strong inclination to early fatigue failure under cyclic loading conditions well below the yield stress, e.g., 10–50% of the stress required for rapid yielding via the formation of shear bands.[2] Macroscopic cyclic loading tests from both experiments[3,4] and molecular dynamics (MD) simulations[5] have been used to characterize cyclic plasticity in metallic glasses, and suggest that the degree of structural relaxation (e.g., free volume content and residual stress) may play an important role in the fatigue of metallic glasses. However, it remains unclear how the damage initiates locally and evolves in the vicinity of a stress concentration.

More recently, nanoindentation has also been used for precision studies of cyclic deformation in metallic glass below the global yield point.[6–8] Specifically, several cycles of loading and unloading are applied at small amplitudes in the nominal elastic range, prior to a final large monotonic indentation that triggers yield. It has been reported from these studies that metallic glasses can be hardened by such cyclic loading processes; statistically, the load required to trigger the first shear band can be significantly increased by cycling.[6] This hardening effect is developed progressively over several cycles, and eventually saturates. Another important characteristic of the cyclic hardening effect is that there exists a threshold of the cycling amplitude, below which no

hardening will result.[6–8] Shear transformation zone dynamics simulations[7] confirmed that under such experimental conditions, confined microplasticity in local regions can occur, and it has been inferred that significant permanent changes to the glass structure (e.g., local coordination, chemical short range order, etc.) must also attend this microplasticity.

The goal of the present work is to use MD simulations to investigate the possible microplasticity-associated, atomic-scale structural changes that lead to cyclic hardening in metallic glass. The simulations are specifically designed to compare with experimental observations based on nanoindentation, and provide the first atomistic view of the hardening mechanism, which has been speculated upon but not yet elucidated in any prior work.

As shown in Fig. 1(a), a three dimensional slab of $Cu_{63.5}Zr_{36.5}$ was constructed and studied by MD following the procedures developed by Shi and Falk.[9] The interatomic interactions were characterized by an embedded atom method (EAM) potential developed by Mendelev *et al.*[10]
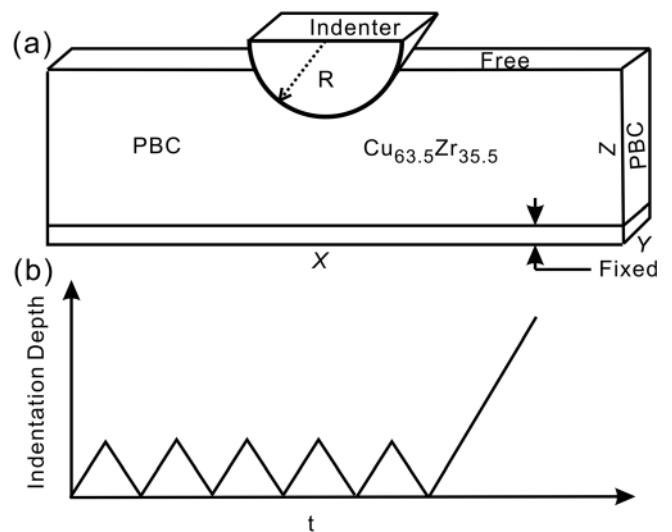

FIG. 1. Schematic of (a) the nanoindentation geometry and (b) the triangular loading function. Periodic boundary conditions are applied along X and Y directions in (a).

a)E-mail: dengc@ad.umanitoba.ca.

100, 251909-1

The binary Cu-Zr metallic glass was chosen because it has been widely studied by both experiments[10,11] and atomistic simulations[10] in the past. Moreover, this particular EAM potential was used because it has been fitted to accurately predict important properties of Cu-Zr, including the glass transition temperature, melting point, bulk modulus, etc.[10] The open source code LAMMPS (Ref. 12) was used for all simulations with a time step of 5 *fs*. The metallic glass sample was prepared by first heating a crystalline mixture of $Cu_{63.5}Zr_{36.5}$ to a temperature of T = 2000 K for 500 *ps*, then quenching to T = 10 K at a constant rate over 2 ns. The pressure was kept at zero during all these steps by applying an isobaric ensemble according to a Nose-Hoover thermostat. The dimensions of the simulation box were {L_X, L_Y, L_Z}: {41.4, 1.2, 11.4} nm. Periodic boundary conditions were applied along the X and Y directions, while the sample surface (along Z) was kept free. Several atom layers at the bottom (along Z) were fixed (Fig. 1(a)). Nanoindentation loading was simulated by moving a cylindrical virtual indenter at a constant velocity of 5 m/s along the Z direction towards the free sample surface (Fig. 1(a)). A repulsive force was exerted by the indenter according to the following equation:

$$p(r) = K(r - R)^2, \qquad (1)$$

where $p(r)$ is the repulsive force, R is the radius of the cylindrical indenter, r is the distance from the atom to the center axis of the cylindrical indenter, and K is the specified force constant. Here, R is set to be 10 nm, and K is 100 eV·nm^{-1}. An isothermal-isobaric ensemble (NPT) was maintained during the indentation process (with pressure $P = 0$ and temperature T = 10 K). A triangular loading function was followed, as shown in Fig. 1(b). Five identical cycles of loading and unloading with relatively small amplitude were applied prior to a sixth, larger loading sufficient to cause global yielding. Three cycling amplitudes (in terms of indentation depth h) have been studied, namely 0.5, 0.6, and 0.7 nm. In order to capture the stochastic nature of the yielding behavior in metallic glass, 40 simulations with different initial thermal conditions (all other simulation conditions are identical) have been carried out at each cycling amplitude.

Typical p-h (p: loading force, h: indentation depth) curves under various conditions are shown in Fig. 2(a). The origin of some of the curves has been shifted for better illustration. The characteristics of the p-h curves agree well with those observed in experiments. For example, the onset of global plasticity is marked by the first discrete event on otherwise smooth curves. In these simulations, the discrete event is a load drop (since the indenter displacement is controlled) where most experiments use load control and record "pop-in" events that are equivalent. Vertical dashed lines are added in Fig. 2(a) to indicate the elastic limit, or the first discrete event, for all simulated cases. The typical atomistic configurations that correspond to the yield events are also included in Fig. 2(b), e.g., (ii) for the yielding in the as-quenched sample with no cycling and (iii) for the yielding in the sample cycled with an amplitude of 0.7 nm, respectively. These snapshots were cropped from the region beneath the indenter, and the atoms were colored by their
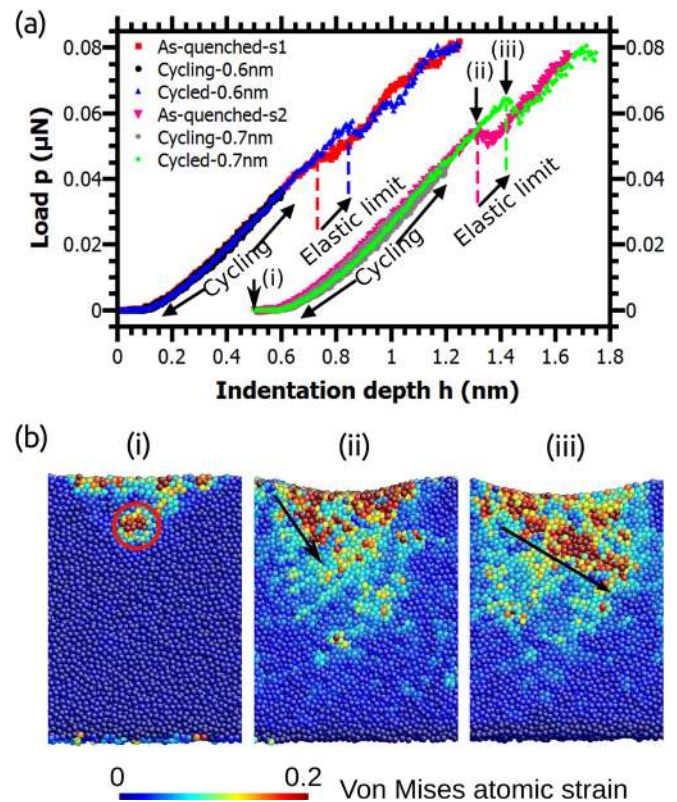

FIG. 2. (a) *p-h* curves in both as-quenched and cycled Cu-Zr metallic glass with amplitude equal to 0.6 and 0.7 nm, respectively. The elastic limit is indicated by a dashed line in each case. The origin for curves with amplitude equal to 0.7 nm has been shifted for better presentation. Vertical arrows correspond to the points immediately after (i) the 5th cycle, (ii) the elastic limit in the as-quenched sample, and (iii) the elastic limit in the sample after cycling with amplitude equal to 0.7 nm, respectively. (b) Snapshots cropped from the region beneath the indenter, showing the atomistic configurations corresponding to points (i), (ii), and (iii) in (a). Black arrows and red circle are added for highlighting purposes. The atom colors correspond to their local von Mises strain (see Ref. 13).

local von Mises strain.[13] Although no large and well-developed shear band was observed at these yield events as in experiments, each strain burst was associated with a localized plastic shear event, as indicated by the red atoms. Black arrows are added in these snapshots to help visualize the direction of displacement for each strain burst. In addition, a snapshot showing the typical atomistic configurations of a simulated sample after 5 cycles of loading and unloading at an amplitude of 0.7 nm is presented in Fig. 2(b) (i). The red atoms highlighted in the red circle indicate that irreversible microplasticity in a confined region underneath the indenter has been progressively developed after nominal elastic cycling, although no observable global residual strain can be detected.

To better demonstrate the effects of cycling upon yield in metallic glass, the yield loads which correspond to the elastic limits as shown in Fig. 2(a) in all simulated samples are summarized in Fig. 3(a) in the form of cumulative distribution functions. Each data point on Fig. 3(a) shows the fraction of yield loads within a certain range among the 40 simulations at each cycling condition. There is a broad distribution of yield load regardless of the loading conditions, which is in line with experimental observations.[6–8] In experiments, it has been shown that such distributions arise
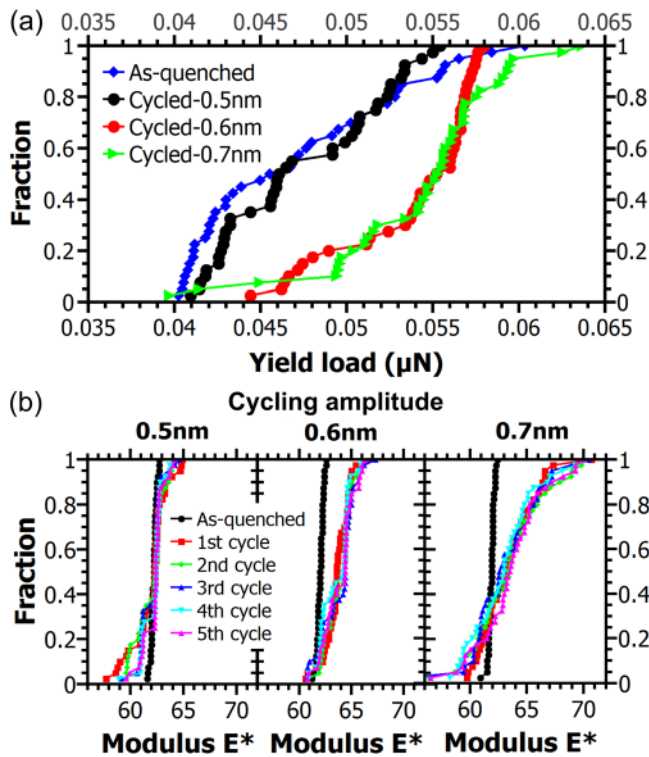
FIG. 3. Cumulative distribution functions of the (a) yield load and (b) reduced modulus E^* in metallic glass under different loading conditions.

due to noise both in the structure of the glass among many different indentation sites, as well as thermal noise;[8] in the present simulations where the structure is not variable, the thermal noise is responsible for the distribution.

There are several interesting points revealed by comparing the p-h curves, the yield loads, and the atomistic configurations at different cycling amplitudes. First, Fig. 3(a) shows clearly that, statistically, the cycling amplitude has to exceed a certain threshold in order to cause hardening effects. For instance, Fig. 3(a) shows that five cycles of indentation at an amplitude of 0.5 nm cause no apparent hardening effect when compared to the as-quenched sample; the yield distributions for the as-quenched and cycled samples overlaps each other. Nonetheless, when the cycling amplitude is increased to 0.6 and 0.7 nm, as shown in both Figs. 2(a) and 3(a), there is a significant increase of the elastic limit/yield load caused by the cycling; the median of the yield loads estimated from Fig. 3(a) shifts from a value around 0.045 μN for the as-quenched to about 0.055 μN for the cycled samples.

For all curves in Fig. 2(a), the cycling is found to be convincingly elastic, as the unloading curves return to the original starting point without any apparent global residual strain even when inspected at the finest scales. It is reasonable, since in both of these cases the cycling amplitude (0.60 and 0.70 nm, respectively) is far below the elastic limit indicated in Fig. 2(a). However, it is interesting to note that in the case with cycling amplitude equal to 0.7 nm, there is significant hysteresis during the cycling, causing the loading and unloading curves to slightly deviate from one another. This finding, together with the atomistic snapshot as shown in Fig. 2(b) (i), thus corroborates the claim that confined microplasticity has occurred during nominally elastic cycling, although no global damage could be observed.

Whereas past experimental work has suggested local stiffening due to possible structural changes, e.g., local crystallization, during the nominal elastic cycling that caused the hardening,[6–8] it has never been directly observed. This study thus provides support for the kinematic irreversibility of cyclic loading in metallic glasses.

The above observations are in excellent qualitative agreement with experimental observations on the cyclic hardening effects in metallic glass. For example, the existence of an apparent elastic regime stable upon cycling and the fact that hardening occurs on cycling in the nominal elastic regime[6–8] have both been observed in experiments. Moreover, the existence of an apparent threshold amplitude for cyclic hardening has also been found experimentally in several different kinds of metallic glasses.[6–8] Although these simulations therefore match the general observations of experiment on various metallic glasses, the more important findings of this work pertain to the ability of MD to reveal the mechanism of cyclic hardening. Specifically, cyclic loading leads to the selection of a secondary path for the strain burst or shear localization at the global yield point; different paths, locations, and directions can be clearly seen from the atomistic snapshots in Fig. 2(b), and this is a general result seen in other simulations as well with different loading rates, temperatures, indenter, and sample sizes (not shown). Since shear localization through a complex multiaxial stress field (like that beneath an indenter) occurs along a path upon which the stress at every point exceeds the yield stress,[14] prior authors[6,7,14] have speculated that cyclic loading may effectively harden some small portion of the originally preferred shear band path, so that the yield must proceed along a secondary path which requires a higher load. Such local hardening would obviously require a significant structural change underneath the indenter after cycling. The results in Fig. 2(b) seem to support the hypothesis that the cycling may have locally hardened some regions of the originally preferred shear band path, since it leads directly to a higher load being required to trigger a secondary path for yielding.

With this observation, we may proceed to more rigorously test this hypothesis. Although strength and hardness are complex properties that speak to the resistance of a large ensemble of atoms to undergo plastic yield (via shear localization), it is a convenient fact that the strength of glassy metals is, to a very good approximation, controlled by their elastic properties; metallic glasses seem to have a common yield strain, with yield strengths differentiated in proportion to their shear moduli.[1] Therefore, one way to reasonably assess local strengthening in the simulated structure is to probe the modulus.

As established by Hertz[15] and Oliver and Pharr,[16] the elastic response of the load-displacement (p-h) curve for indentations on metallic glass can be predicted by:

$$p = E^* \cdot h^m, \tag{2}$$

where m and E^* are fitting parameters that relate to the modulus and geometry of both the tested material and indenter. For simulations in this study, E^* can be treated as a reduced modulus that reflects the modulus of the indented metallic

glass, because all other parameters, e.g., the indenter modulus and size, are identical regardless the loading conditions. To assess cycling effects on the modulus of simulated metallic glass, Fig. 3(b) summarizes the values of E^* in the form of a cumulative distribution function. Here, E^* was obtained by fitting the data points on all the p-h curves by Eq. (2) up to an indentation depth of 0.5 nm to ensure that only elastic responses have been fitted. m is fixed at a value of 1.5 to be consistent with experiments.[6–8]

The plots in Fig. 3(b) show clear trends: E^* changes as a result of cycling at different amplitudes, which matches the cycling effects on yield load as shown in Fig. 3(a); While a cycling amplitude of 0.5 nm has little effect on E^*, statistically, 5 cycles of loading and unloading at amplitudes of 0.6 and 0.7 nm have significantly shifted E^* towards the higher end. It is also worth noting that the curves in Fig. 3(b) reflect a saturation of cyclic hardening, in that the curves for the last several cycles almost overlap each other. This is consistent with experimental observations that hardening effects saturate after a certain number of cycles (about 5-10).[6–8]

One interesting question not explicitly resolved here is the nature of the structural change that causes local hardening. We have employed many of the most common tools of glass structure evolution, including free volume evolution,[17] chemical short range ordering,[18] local coordination analysis by radial distribution function,[19] and atomic packing (e.g., distribution of different types of polyhedra) based on Voronoi analysis.[20] None of these methods were found to reveal any clear signal of change induced by cycling. Cyclic structure evolution in metallic glasses is thus not only subtle at the scale of experimental methods, but at the atomic scale as well. Progress on this topic may await better measures and classifications of the glass structure itself.

In summary, MD simulations have been used to study cyclic plasticity in Cu-Zr metallic glass under nanoindentation within the nominal elastic regime. The simulations not only properly reflect the characteristics of cyclic hardening observed in experiments, they also reveal that the hardening is connected with atomic level structural changes and microplasticity within confined regimes. These simulations thus support the hypothesis that cyclic loading hardens the primary yielding path in a metallic glass, thus forcing yield to occur on a secondary path at a higher applied load.

[1]C. A. Schuh, T. C. Hufnagel, and U. Ramamurty, Acta Mater. **55**, 4067 (2007).

[2]B. C. Menzel and R. H. Dauskardt, Scr. Mater. **55**, 601 (2006).

[3]M. E. Launey, R. Busch, and J. J. Kruzic, Scr. Mater. **54**, 483 (2006).

[4]M. E. Launey, R. Busch, and J. J. Kruzic, Acta Mater. **56**, 500 (2008).

[5]Y. C. Lo, H. S. Chou, Y. T. Cheng, J. C. Huang, J. R. Morris, and P. K. Liaw, Intermetallics **18**, 954 (2010).

[6]C. E. Packard, L. M. Witmer, and C. A. Schuh, Appl. Phys. Lett. **92**, 171911 (2008).

[7]C. E. Packard, E. R. Homer, N. Al-Aqeeli, and C. A. Schuh, Philos. Mag. **90**, 1373 (2010).

[8]C. E. Packard, O. Franke, E. R. Homer, and C. A. Schuh, Journal of Materials Research **25**, 2251 (2010).

[9]M. L. Falk and Y. F. Shi, Acta Mater. **55**, 4317 (2007).

[10]M. I. Mendelev, M. J. Kramer, R. T. Ott, D. J. Sordelet, D. Yagodin, and P. Popel, Philos. Mag. **89**, 967 (2009).

[11]D. Wang, Y. Li, B. B. Sun, M. L. Sui, K. Lu, and E. Ma, Appl. Phys. Lett. **84**, 4029 (2004).

[12]S. Plimpton, J. Comput. Phys. **117**, 1 (1995).

[13]J. Li, Modell. Simul. Mater. Sci. Eng. **11**, 173 (2003).

[14]C. E. Packard and C. A. Schuh, Acta Mater. **55**, 5348 (2007).

[15]H. Hertz, *Miscellaneous Papers* (Macmillan, London, 1896).

[16]W. C. Oliver and G. M. Pharr, J. Mater. Res. **7**, 1564 (1992.)

[17]T. Eagmi and D. Srolovitz, J. Phys. F: Met. Phys. **12**, 2141 (1982).

[18]A. C. Lund and C. A. Schuh, Phys. Rev. Lett. **91**, 235505 (2003).

[19]D. S. Boudreaux, Phys. Rev. B **18**, 4039 (1978).

[20]J. Park and Y. Shibutani, Mater. Trans. **47**, 2904 (2006).